Publishing Excellence
Inspiring Progress
ARISTON PUBLICATIONS
MatSci Express
ISSN: 2997-8440 www.aristonpubs.com/matsci-express https://doi.org/10.69626/mse.2026.0120

RESEARCH ARTICLE

Simulation of Spin–Dependent Quantum Magnetometry for Weak Geomagnetic Field Detection Using Optically Detected Magnetic Resonance

Gul Faroz Ahmad Malik[1], Hilal Ahmad Bhat[2], Samiya Shah[3], C. A. Duque[4]

ABSTRACT: Detecting weak magnetic fields is important for geophysics, navigation, space weather monitoring, and quantum sensing. This study presents a simulation-based framework for a spin-dependent quantum magnetometer operating within the geomagnetic field range. The model represents an effective two-level spin defect and relates Zeeman splitting to optically detected magnetic resonance (ODMR). A Lorentzian resonance profile incorporates spin coherence decay, linewidth broadening, and Gaussian noise. Simulations across magnetic fields of 25–65 μT, using nitrogen-vacancy center-like parameters, demonstrate a linear relationship between resonance frequency and magnetic field. Longer transverse relaxation times produce narrower resonances and improve sensitivity, whereas noise reduces the signal-to-noise ratio. Nevertheless, the resonance remains resolvable under the investigated conditions. A noise-to-slope estimation method predicts room-temperature magnetic sensitivity in the nanotesla range, consistent in order of magnitude with reported solid-state quantum magnetometers. These findings highlight the potential of spin-based quantum magnetometry for geomagnetic sensing and provide a computational foundation for optimizing coherence, linewidth, and noise before device fabrication.

Keywords: Spin-based quantum sensing; Geomagnetic field detection; Optically detected magnetic resonance; Zeeman splitting; Magnetic sensitivity; Spin coherence.

Received: 07 June 2026; Revised: 17 June 2026; Accepted: 05 July 2026; Published Online: 01 August 2026

1. INTRODUCTION

Detecting weak magnetic fields with high precision is a foundational requirement across several scientific and technological domains, including geophysics, navigation, space science, and Earth observation systems [1, 2]. The geomagnetic field, which naturally varies in the range of tens of microtesla, carries a wealth of information that is critical for geomagnetic mapping and positioning. Conventional magnetometers, such as Hall-effect and fluxgate sensors, are widely deployed for these purposes [3, 4]. However, their sensitivity and scalability are often constrained by intrinsic noise sources and practical device limitations, which has motivated a sustained search for alternative sensing modalities. Recent progress in quantum technologies has established that spin-based systems can function as highly sensitive probes of magnetic fields [5, 6]. The direct coupling of magnetic fields to spin states through the Zeeman interaction enables spin-state-based quantum magnetometers

[1] Department of Electronics and I.T., University of Kashmir, Hazratbal, Srinagar, Jammu and Kashmir, India
[2] Department of Physics, Mahindra University, Hyderabad, Telangana, India
[3] Department of Electrical Engineering, Institute of Technology, University of Kashmir, Srinagar, 190006, India
[4] Grupo de Materia Condensada-UdeA, Instituto de Física, Facultad de Ciencias Exactas y Naturales, Universidad de Antioquia UdeA, Calle 70 No. 52-21, Medellín AA 1226, Colombia

* Author to whom correspondence should be addressed: gfarozam@gamil.com (G. F. A. Malik)

© Ariston Publications 2026. All rights reserved.

to achieve enhanced sensitivity [7]. Solid-state spin platforms, which include defect spins in wide-bandgap semiconductors and spin-dependent transport devices, have attracted considerable attention because of their potential for miniaturization, room-temperature operation, and device-level integration [8].

Among the various approaches, optically detected magnetic resonance (ODMR) has emerged as one of the most effective techniques for converting magnetic-field-induced spin transitions into signals that can be measured using conventional electronic principles [9, 10]. In this scheme, the resonant frequency of a spin system varies linearly with the applied magnetic field, providing a direct route to quantitative field estimation. The performance of such spin-based quantum magnetometers is strongly governed by the spin coherence properties of the system, as the resonance linewidth and the noise floor together determine the achievable magnetic sensitivity [11, 12]. Although experimental efforts have made substantial progress, systematic simulation studies that integrate spin-physics effects, noise contributions, and sensitivity estimation under geomagnetic field conditions remain relatively limited [13], [14]. In particular, device-oriented modeling that connects fundamental spin responses to actual geomagnetic sensing performance is essential for the rational design and optimization of spin-based quantum magnetometer devices. The model parameters adopted in this work are consistent with nitrogen-vacancy (NV) center-like spin defects in diamond, which are among the most widely studied systems for ODMR-based quantum magnetometry.

Despite the growing body of experimental work on NV-center magnetometry, there remains a notable gap in the literature regarding comprehensive simulation frameworks that specifically address the geomagnetic field regime while simultaneously incorporating the combined effects of spin coherence decay, realistic noise sources, and device-level sensitivity metrics. Most existing simulation studies either focus on idealized conditions that neglect noise or operate in field ranges that are not representative of Earth's magnetic environment. This work addresses that gap by developing a simulation-based framework that explicitly targets the 25–65 μT geomagnetic range and evaluates magnetic sensitivity through a noise-to-slope estimation method that accounts for Gaussian noise contributions. The novelty of the present study lies in its integration of Zeeman splitting, Lorentzian ODMR line shape modeling, coherence-limited linewidth broadening, and noise-limited sensitivity estimation into a single device-oriented framework that can serve as a design tool for spin-based quantum magnetometers prior to fabrication.

In this paper, we report a spin-based quantum magnetometer device simulation model that operates in the geomagnetic field regime. The model incorporates the Zeeman splitting of spin states, ODMR signal formation, spin coherence decay, and noise contributions into the evaluation of magnetic sensitivity. Given the focus on Earth-scale magnetic fields, this work aims to provide a theoretical framework for understanding the noise-limited performance of spin-device-based quantum magnetometers and to assess their feasibility for geomagnetic field sensing applications. The paper is organized as follows: Section 2 introduces the physical background. Section 3 provides the simulation methodology. Section 4 presents the results and discussion. The paper is concluded in Section 5.

2. PHYSICAL BACKGROUND

2.1. Spin–Magnetic Field Interaction and Zeeman Splitting

The interaction between the spin system and the external magnetic field forms the fundamental operating principle of spin-based quantum magnetometers. For an effective spin $\frac{1}{2}$ system subjected to an external magnetic field B, the Zeeman Hamiltonian is written as [15]:

$$\widehat{H_Z} = g\ \mu_B\ B\widehat{S}, \tag{1}$$

Where g is the Lande g-factor, μ_B the Bohr magneton, and $\hat{S}$ the spin operator.

The NV center is approximated here as an effective two-level spin system in order to capture the dominant ODMR response under weak geomagnetic-field conditions. Although more complete multi-level descriptions may include angular anisotropies and spin-state mixing, the present approximation is sufficient for the qualitative sensitivity analysis considered in this work. In the presence of an applied magnetic field along the direction of the quantization axis, the spin energy levels split into two distinct states, the resulting energy separation can be written as;

$$\Delta E = g\ \mu_B\ B\ . \tag{2}$$

This Zeeman splitting gives rise to a magnetic-field-dependent transition frequency,

$$f(B) = \frac{\Delta E}{h} = \frac{g\mu_B B}{h}\ , \tag{3}$$

Where h is Planck's constant. At geomagnetic field strengths, which are typically 25 to 65 μT, this frequency shift lies in the radio-frequency or microwave range of the electromagnetic spectrum and can be accurately detected using existing resonance-based techniques [2, 10].

2.2. Optically Detected Magnetic Resonance (ODMR)

ODMR provides a highly efficient readout mechanism for spin-based quantum magnetometers [2, 6]. It converts spin-state transitions into measurable signals, which can be either optical or electrical signals. When a microwave field with frequency f is applied, resonance occurs at $f \approx f(B)$, resulting in a change in the detected signal intensity. The ODMR response can be modeled using a Lorentzian line shape [16];

© Ariston Publications 2026. All rights reserved.

$$S(f) = 1 - \frac{C}{1+\left(\frac{f-f_0}{\Gamma}\right)^2}, \quad (4)$$

Where C is the contrast of resonance and f_0 is the magnetic field-dependent resonance frequency. The linewidth of the resonance is represented by Γ. The shift of $f0$ with the magnetic field provides the basis for magnetic field estimation in quantum magnetometers.

2.3. Spin Coherence and Decoherence Effects

The coherence properties of the spin system influence the sensitivity of a spin-based quantum magnetometer [11, 12]. Spin coherence is characterized by the transverse relaxation time T_2, which quantifies the decay of phase coherence due to interactions with the magnetic field in the surrounding environment. The temporal decay of spin coherence can be described as [17];

$$C(t) = e^{\frac{t}{T_2}}, \quad (5)$$

Where t stands for evolution time. If the coherence time is short, it will lead to broader resonance linewidths and reduced signal contrast, which, in turn, degrade magnetic sensitivity. Therefore, spin coherence plays a critical role in determining the performance limits of quantum magnetometer devices.

2.4. Noise and Magnetic Sensitivity Estimation

In practical sensing settings, noise affects the ODMR signal through both fundamental and technical sources. The magnetic sensitivity δ_B is defined as the minimum detectable change in magnetic field [18]. It can be estimated using the noise-to-slope ratio,

$$\delta_B = \frac{\delta S}{\left|\frac{dS}{dB}\right|}, \quad (6)$$

Where δ_S is the root-mean-square (RMS) noise in the detected signal, and the slope of the signal with respect to the magnetic field is represented by $\frac{dS}{dB}$. The slope can be written using the chain rule and can be expressed as [19];

$$\frac{dS}{dB} = \frac{dS}{df} \cdot \frac{df}{dB}, \quad (7)$$

Where, $\frac{df}{dB} = \gamma$, which is the gyromagnetic ratio of the spin system. This mathematical formula enables direct estimation of magnetic sensitivity from the simulated ODMR response. This provides a quantitative measure of device performance under geomagnetic field surroundings.

2.5 Spin-FET Response under Geomagnetic Field

The response of a spin field-effect transistor (Spin-FET) to the geomagnetic field is modeled by considering the magnetic-field-dependent spin polarization of charge carriers. The spin polarization is expressed as [20];

$$P(B) = P_0 \cos(\alpha B), \quad (8)$$

Where P_0 is the maximum spin polarization, and α represents the magnetic coupling factor. The drain current of the Spin-FET is assumed to depend linearly on the spin polarization and is given by [21];

$$I(B) = I_0(1 + P(B)), \quad (9)$$

Where I_0 is the baseline drain current in the absence of spin polarization. The simulated results show that variations in the geomagnetic field of 25–65 μT produce measurable modulations in the drain current, demonstrating the sensitivity of spin-dependent transport to weak magnetic fields. This behavior demonstrates that even under Earth-scale magnetic fields, measurable electrical signatures can be obtained, supporting the feasibility of using Spin-FET devices as compact electronic readout components in spin-based quantum magnetometer systems.

3. SIMULATION METHODOLOGY

To model the response of a spin-based quantum magnetometer device under geomagnetic field conditions, a simulation methodology was developed in this work. The methodology incorporates analytical spin physics and numerical evaluation to estimate magnetic sensitivity in the presence of noise. All simulations were implemented using the mathematical models, and the results were computed in MATLAB. The calibrated simulations account for magnetic fields in the range of the typical geomagnetic field, 25–65 μT. The spin system is considered by an effective g = 2 electron g-factor, corresponding to a gyromagnetic ratio (γ) of 28 GHz.T^{-1}. The zero-field resonance frequency (f_{ZFS}) is taken as 2.87 GHz, consistent with frequently reported spin-defect systems. The ODMR linewidth (Γ) and contrast (C) are treated as adjustable parameters to assess their influence on the modeled sensor's performance. Spin coherence effects are combined through an effective transverse relaxation time T_2, which governs resonance widening.

For the modeling of ODMR signal, if the given magnetic field is B, the resonance frequency is:

$$f_0(B) = f_{ZFS} + \gamma B. \quad (10)$$

The ODMR signal is modeled using a Lorentzian dip centered at $f_0(B)$,

$$S(f) = 1 - \frac{C}{1+\left(\frac{f-f_0}{\Gamma}\right)^2}. \quad (11)$$

© Ariston Publications 2026. All rights reserved.

Table 1. Simulation parameters used in the spin-based quantum magnetometer model.

Parameter	Symbol	Value	Unit	Description
Geomagnetic field range	B	25–65	μT	Earth's magnetic field range
Landé g-factor	g	2		Effective electron g-factor
Gyromagnetic ratio	γ	28×10^9	Hz/T	Spin gyromagnetic ratio
Bohr magneton	μ_B	9.274×10^{-24}	J/T	Fundamental magnetic constant
Planck constant	h	6.626×10^{-34}	J·s	Fundamental constant
Zero-field resonance frequency	f_{ZFS}	2.87×10^9	Hz	Zero-field splitting
ODMR linewidth	Γ	$1\text{-}3 \times 10^6$		Resonance linewidth
ODMR contrast	C	0.2-0.4		Relative signal contrast
Spin coherence time	T_2	0.5-2	μs	Transverse relaxation time
Noise standard deviation	δ_S	0.005-0.02		RMS signal noise
Frequency sweep range	f	2.86-2.88	GHz	Microwave scan range
Frequency resolution	Δf	$\sim 10^4$	Hz	Frequency step size

To generate the ODMR spectrum, a microwave frequency sweep is performed around the resonance. This formulation captures the essential magnetic-field-dependent effects required for quantum magnetometer operation. Furthermore, for the incorporation of spin coherence effect, the linewidth parameter Γ is introduced, which is related to the coherence time T_2 as;

$$\Gamma = \frac{1}{\pi T_2} \ . \tag{12}$$

By varying T_2, the influence of coherence decay on resonance sharpness and signal slope is examined. This allows assessment of how coherence limitations affect magnetic sensitivity.

Finally, under realistic sensing conditions, noise is modeled by adding noise to the simulated ODMR signal. The noise is assumed to be Gaussian-distributed, representing a combination of shot noise and technical noise sources. The noisy signal is expressed as:

$$S_{noisy}(f) = S(f) + \delta S, \tag{13}$$

Where δ_S is a random noise term with zero mean and a specified standard deviation. The root-mean-square (RMS) noise level is extracted directly from the simulated data and used in sensitivity calculations.

Magnetic Sensitivity Estimation: Magnetic sensitivity is evaluated using the noise-to-slope method. The frequency derivative of the ODMR signal is computed numerically,

$$\frac{dS}{df} = \frac{S(f_{i+1}) - S(f_i)}{f_{i+1} - f_i} \tag{14}$$

and converted into a magnetic-field derivative using the relation:

$$\frac{dS}{dB} = \frac{dS}{df} \cdot \gamma \ . \tag{15}$$

The minimum detectable magnetic field variation is then obtained as:

$$\delta B = \frac{\delta S}{max\left(\left|\frac{dS}{dB}\right|\right)} \ . \tag{16}$$

This procedure provides a quantitative estimate of the noise-limited sensitivity of the spin-based quantum magnetometer device under geomagnetic field conditions. The simulation parameters used in the spin-based quantum magnetometer model are given in Table 1.

The Spin-FET framework is included here as a complementary spin-transport perspective that may be relevant for future hybrid quantum sensing architectures integrated with ODMR-based platforms.

4. RESULTS AND DISCUSSION

4.1. Linear Zeeman response and ODMR line shape

The simulated resonance frequency exhibits a linear dependence on the applied magnetic field within the geomagnetic range of 25 to 65μT. This behavior comes from the Zeeman splitting in the spin states and is in agreement with the relation:

$$f_0(B) = f_{ZFS} + \gamma B \ . \tag{17}$$

Because the response remains linear, the sensor operates in the weak-field regime, where higher-order magnetic interactions are negligible. The corresponding frequency shift lies within the microwave band, which means that Earth-scale field variations can be resolved using standard resonance techniques. The simulated shift is consistent with the gyromagnetic ratio of 28 GHz T−1 and the zero-field splitting of 2.87 GHz used in the model. This confirms that the effective two-level approximation captures the dominant physics required for geomagnetic field sensing. Figure 1 presents a representative ODMR spectrum. A well-defined resonance dip appears at the magnetic-field-dependent frequency. In the absence of noise, the Lorentzian profile is

© Ariston Publications 2026. All rights reserved.

sharp and the contrast is high. When Gaussian noise is added, the dip remains identifiable, but the effective signal-to-noise ratio decreases. This behavior shows that ODMR readout is robust under realistic noise levels, while also making clear that noise suppression is essential for improving sensor performance. The simulated contrast values between 0.2 and 0.4 are sufficient to preserve the resonance feature even when the RMS noise reaches 0.02. The results therefore support the use of ODMR as a reliable readout mechanism for weak-field quantum magnetometry.

4.2. Influence of spin coherence on linewidth and signal slope

The effective coherence time T2 was varied to examine how spin coherence affects the ODMR response, as shown in Figure 2. A short T2 broadens the resonance linewidth and reduces the slope at the resonance point. Since the slope determines how strongly the signal changes with magnetic field, this broadening directly degrades magnetic sensitivity. Longer coherence times produce narrower resonances and higher contrast. The linewidth is related to T2 through $\Gamma = 1/(\pi T2)$, so coherence decay is not a secondary effect but a primary factor that sets the achievable resonance sharpness. For the T2 range of 0.5 to 2 μs used here, the corresponding linewidths fall between roughly 1 and 3 MHz. These values are consistent with room-temperature NV-center behavior. The analysis shows that extending T2 through material improvement, defect engineering, or optimized device geometry is one of the most effective ways to improve spin-based magnetometer performance.

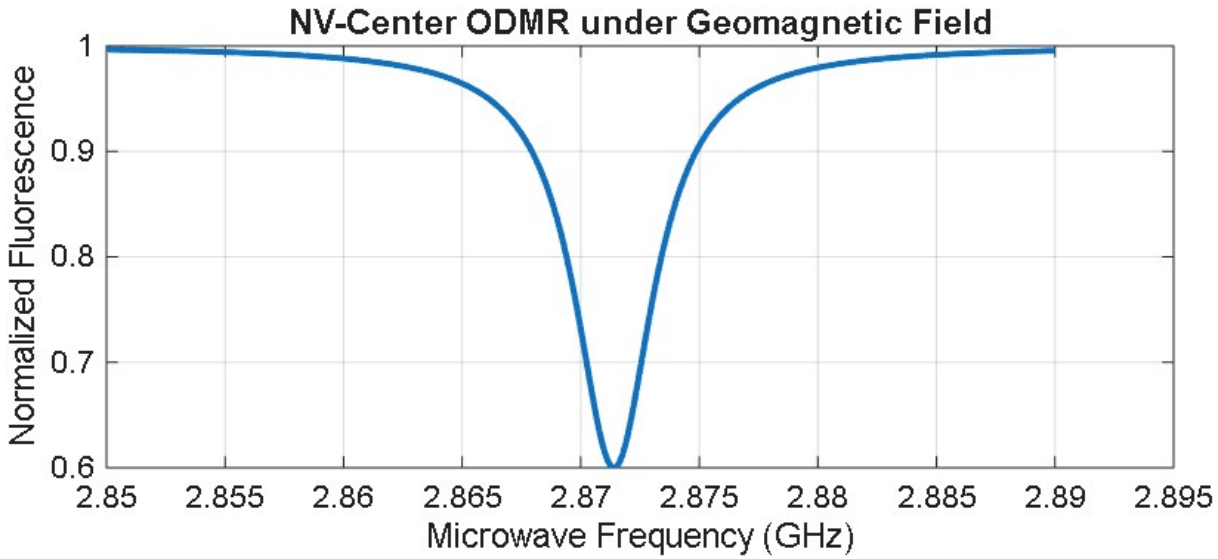

Fig. 1. Simulated ODMR spectrum of an NV-center-like spin system under a typical geomagnetic field.

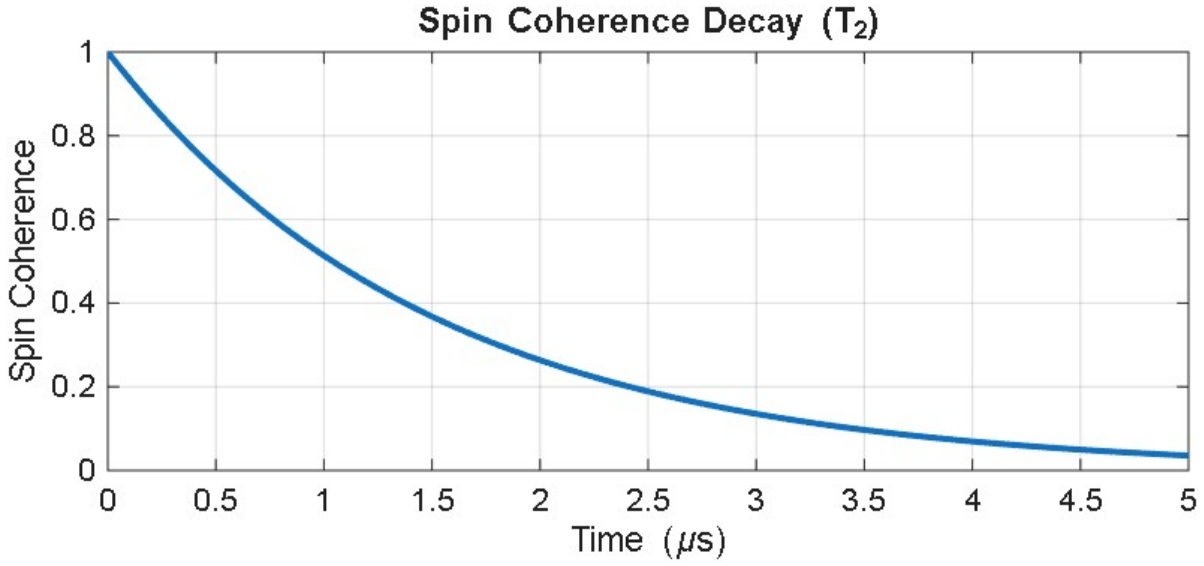

Fig. 2. Spin coherence decay as a function of evolution time for the effective transverse relaxation time T2.

© Ariston Publications 2026. All rights reserved.

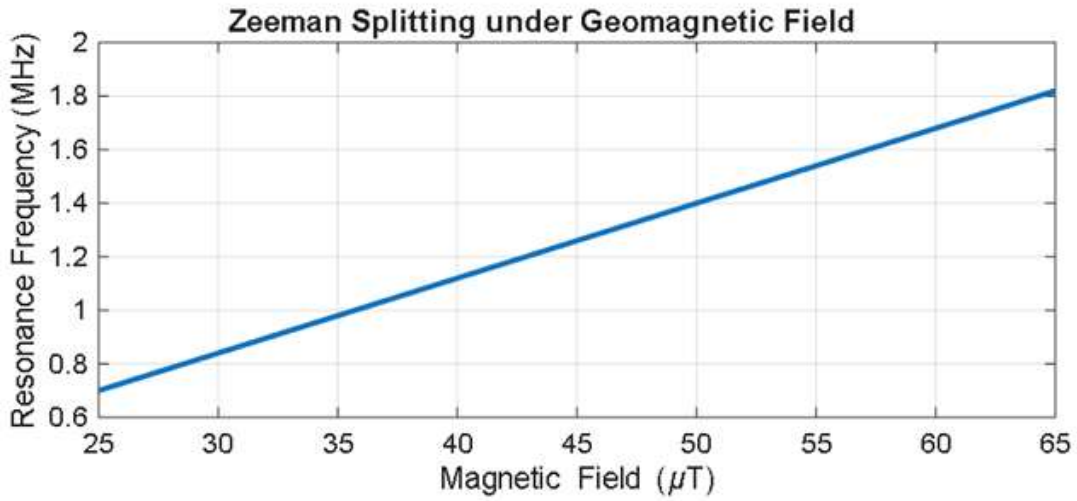

Fig. 3. Effective Zeeman splitting under a geomagnetic field.

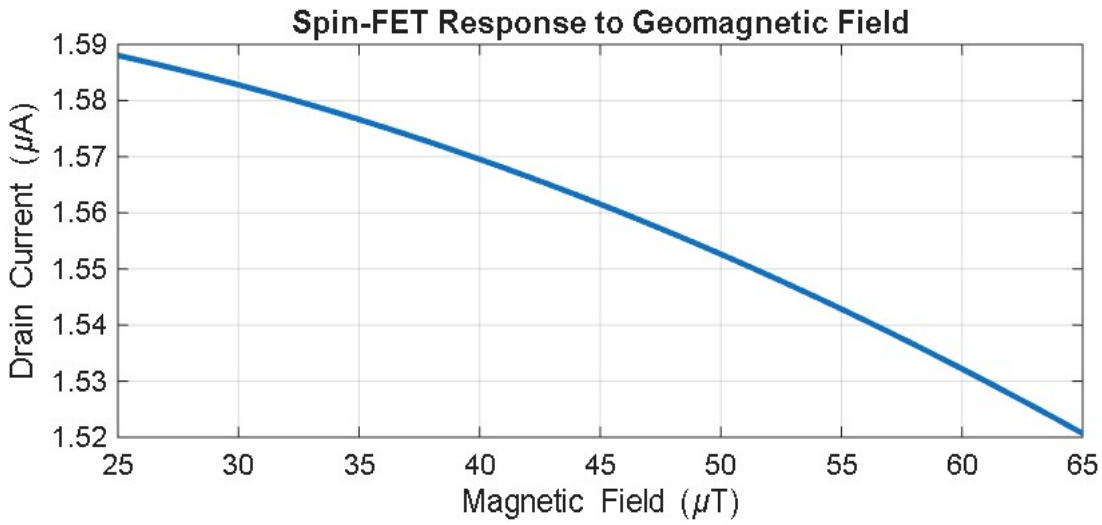

Fig. 4. Spin-FET drain current response to the geomagnetic field.

4.3. Magnetic sensitivity from noise-to-slope estimation

The magnetic sensitivity was evaluated using the noise-to-slope method. The numerical derivative of the ODMR signal with respect to frequency was converted into a magnetic-field derivative using the gyromagnetic ratio (Figure 3). The maximum slope occurs near the resonance frequency, which is where the sensor is most sensitive. Under the calibrated simulation parameters, the estimated sensitivity lies in the nano-tesla range. This level is sufficient to detect variations in the geomagnetic field and is comparable in order of magnitude to reported solid-state quantum magnetometers operating under similar conditions [6, 22]. Figure 3 shows the effective Zeeman splitting under a geomagnetic field. The resonance frequency increases with the applied field, as expected from the linear model. This further supports the consistency of the simulation framework. The noise-to-slope estimate also shows that sensitivity improves when the RMS noise is reduced or when the maximum slope is increased. Since the slope depends on contrast and linewidth, the sensitivity analysis connects directly to the coherence and linewidth results discussed above.

4.4. Spin-FET response and hybrid readout potential

Figure 4 shows the Spin-FET response to the geomagnetic field. The drain current varies smoothly and monotonically with the applied field, following the cosine-dependent spin polarization model $P(B) = P0 \cos(\alpha B)$ and the linear current relation $I(B) = I0\ P(B)$. Within the 25–65 μT range, the drain current decreases gradually as the carrier spin alignment is modulated by the magnetic interaction. Although the current variation is relatively small, it remains clearly distinguishable. This confirms that spin-dependent transport in the Spin-FET is sensitive to weak magnetic fields. The

© Ariston Publications 2026. All rights reserved.

result supports the feasibility of using Spin-FET devices as compact electronic readout components in hybrid spin-based quantum magnetometer systems, where ODMR provides high sensitivity and spin transport provides a route to on-chip electrical integration. The simulated behavior also suggests that spin-transport readout could be combined with ODMR in future hybrid architectures without requiring cryogenic cooling.

4.5. Comparison with reported magnetometers and device-level implications

Table 2 places the present results in context. NV-center quantum magnetometers based on ODMR of spin defects in diamond typically reach about 1–10 nT/√Hz at room temperature [6]. NV ensemble magnetometers use ensemble averaging and can reach pT/√Hz [22]. Optically pumped magnetometers based on atomic spin precession achieve fT/√Hz [5]. SQUID magnetometers also reach fT/√Hz, but require cryogenic operation [23]. Fluxgate magnetometers operate at room temperature with nT-level sensitivity [24], while Hall-effect sensors provide only μT-level sensitivity [3]. The present work, which combines ODMR and spin transport in a simulation framework, predicts nT-level sensitivity at room temperature. The agreement in order of magnitude with reported NV-based sensors supports the validity of the modeling approach and its usefulness for guiding device design and parameter optimization.

The simulation results provide useful insight into the viability of spin-based quantum magnetometer devices for real-world geomagnetic sensing. The linear dependence of resonance frequency on magnetic field and the demonstrated nano-tesla-range sensitivity indicate that such devices can operate effectively within Earth's magnetic field. From a device perspective, the results highlight the critical roles of spin coherence and resonance linewidth. Improving coherence time or reducing linewidth directly increases the signal slope and therefore the magnetic sensitivity. This observation suggests that material quality, defect engineering, and device geometry are key factors in optimizing spin-based quantum magnetometers. The framework also allows rapid estimation of noise-limited performance, which is helpful for comparing design options before fabrication. By quantifying how noise and coherence affect sensitivity, the model can guide trade-off analysis among sensitivity, stability, and device complexity. These considerations are especially relevant for compact, low-power geomagnetic sensors intended for portable devices and embedded applications. Overall, the results suggest that spin-based quantum magnetometer devices offer a worthwhile pathway toward next-generation geomagnetic sensors. The presented modeling approach provides a basis for translating fundamental spin physics into device-level performance metrics, supporting the development and optimization of practical quantum magnetometric sensing technologies.

5. CONCLUSION

This work has presented a simulation-based framework for a spin-dependent quantum magnetometer designed to operate under geomagnetic field conditions. The model brings together the central physical mechanisms that govern spin-based magnetic sensing, namely Zeeman splitting, optically detected magnetic resonance, spin-coherence decay, and noise-limited sensitivity estimation.

Table 2. Comparison of the present simulated spin-based device with reported quantum and classical magnetometers.

Device / Technique	Operating Principle	Typical Sensitivity	Operating Conditions	Ref.	Remarks
NV-center quantum magnetometer	ODMR of spin defects in diamond	~1–10 nT/√Hz	Room temperature	[6]	Benchmark quantum sensor
NV ensemble magnetometer	Ensemble ODMR averaging	~pT/√Hz	Room temperature	[22]	High sensitivity via averaging
Optically pumped magnetometer (OPM)	Atomic spin precession	~fT/√Hz	Vapor cell	[5]	Ultra-high sensitivity
SQUID magnetometer	Superconducting quantum interference	~fT/√Hz	Cryogenic	[23]	Requires low temperature
Fluxgate magnetometer	Core saturation principle	~nT	Room temperature	[24]	Widely used classical sensor
Hall-effect sensor	Lorentz force-based	~μT	Room temperature	[3]	Low sensitivity
This work (Spin-based device)	ODMR + spin transport (simulation)	**~nT**	Room temperature (simulated)	Present work	Compact, device-oriented

© Ariston Publications 2026. All rights reserved.

Across the geomagnetic range of 25 to 65 μT, the simulated resonance frequency follows a linear dependence on the applied magnetic field, which confirms that the system operates in the expected weak-field regime and that higher-order magnetic effects can be neglected. The ODMR spectra show that the resonance remains distinguishable even after Gaussian noise is included, although the effective signal-to-noise ratio is reduced. The analysis further shows that the transverse relaxation time T2 has a strong influence on both resonance linewidth and magnetic sensitivity. Longer coherence times produce sharper resonance profiles and larger signal slopes, which directly improve sensing performance. Under the simulation conditions considered here, the estimated sensitivity reaches the nano-tesla range. This value agrees in order of magnitude with several room-temperature solid-state quantum magnetometers reported in the literature, which supports the validity of the modeling approach. The results emphasize that preserving spin coherence, controlling resonance linewidth, and reducing noise are the most important routes to improved magnetic sensitivity. Overall, the proposed framework offers a practical device-oriented method for evaluating spin-based quantum magnetometers before fabrication and can serve as a useful platform for designing compact quantum sensors for geomagnetic and low-field applications. The complementary spin-transport analysis indicates that hybrid readout schemes may be feasible for compact electronic integration.

DECLARATIONS

Ethical Approval

We affirm that this manuscript is an original work, has not been previously published, and is not currently under consideration for publication in any other journal or conference proceedings. All authors have reviewed and approved the manuscript, and the order of authorship has been mutually agreed upon.

Funding

No Funding

Availability of data and material

All of the data obtained or analyzed during this study is included in this paper.

Conflicts of Interest

The authors declare that they have no financial or personal interests that could have influenced the research and findings presented in this paper. The authors alone are responsible for the content and writing of this article.

Author's contribution statement

Dr. Gul Faroz A. Malik: Conceptualization, Methodology, Software, Investigation, Writing -original draft preparation, Editing, Reviewing. Dr. Hilal A. Bhat: Data curation, Visualization, Investigation, Software, Editing, Revision. Samiya Shah: Data curation, Visualization, Investigation, Original draft preparation. Dr. C. A. Duque: Supervision, Reviewing and Editing, Software-support.

Data availability statement

The data supporting the findings of this study are available from the corresponding author upon reasonable request.

ACKNOWLEDGEMENTS

CAD is grateful to CODI-Universidad de Antioquia (Project: "Nanoestructuras semiconductoras con simetría axial basadas en InAs y GaAs para aplicaciones en electrónica ultra e hiperrápida") and Facultad de Ciencias Exactas y Naturales-Universidad de Antioquia (CAD exclusive dedication project 2026–2027).

REFERENCES

[1] Jacobs, J. A. (**1987**). Geomagnetism, Vol. 1. New York, NY, USA: Academic Press.

[2] Griffiths, D. J. (**2013**). Introduction to Electrodynamics, 4th ed. Boston, MA, USA: Pearson.

[3] Popovic, R. S. (**2004**). Hall Effect Devices, 2nd ed. Boca Raton, FL, USA: CRC Press.

[4] Ripka, P. (**2003**). Advances in fluxgate sensors. Sensors and Actuators A: Physical, 106(1–3), 8–14. https://doi.org/10.1016/S0924-4247(03)00094-3.

[5] Budker, D., & Romalis, M. (**2007**). Optical magnetometry. Nature Physics, 3, 227–234. https://doi.org/10.1038/nphys566.

[6] Taylor, J. M., Cappellaro, P., Childress, L., Jiang, L., Budker, D., Hemmer, P. R., Yacoby, A., Walsworth, R., & Lukin, M. D. (**2008**). High-sensitivity diamond magnetometer with nanoscale resolution. Nature Physics, 4, 810–816. https://doi.org/10.1038/nphys1075.

[7] Degen, C. L., Reinhard, F., & Cappellaro, P. (**2017**). Quantum sensing. Reviews of Modern Physics, 89, 035002. https://doi.org/10.1103/RevModPhys.89.035002.

[8] Dolde, F., Fedder, H., Doherty, M. W., Nöbauer, T., Rempp, F., Balasubramanian, G., Wolf, T., Reinhard, F., Hollenberg, L. C. L., Jelezko, F., & Wrachtrup, J. (**2011**). Electric-field sensing using single diamond

© Ariston Publications 2026. All rights reserved.

spins. Nature Physics, 7, 459–463. https://doi.org/10.1038/nphys1969.

[9] Rondin, L., Tetienne, J.-P., Hingant, T., Roch, J.-F., Maletinsky, P., & Jacques, V. (**2014**). Magnetometry with nitrogen-vacancy defects in diamond. Reports on Progress in Physics, 77, 056503. https://doi.org/10.1088/0034-4885/77/5/056503.

[10] Balasubramanian, G., Chan, I. Y., Kolesov, R., Al-Hmoud, M., Tisler, J., Shin, C., Kim, C., Wojcik, A., Hemmer, P. R., Krueger, A., Hanke, T., Leitenstorfer, A., Bratschitsch, R., Jelezko, F., & Wrachtrup, J. (**2008**). Nanoscale imaging magnetometry with diamond spins under ambient conditions. Nature, 455, 648–651. https://doi.org/10.1038/nature07278.

[11] Zhao, N., Honert, J., Schmid, B., Klas, M., Isoya, J., Markham, M., Twitchen, D., Jelezko, F., Liu, R.-B., Fedder, H., & Wrachtrup, J. (**2012**). Sensing single remote nuclear spins. Nature Nanotechnology, 7, 657–662. https://doi.org/10.1038/nnano.2012.152.

[12] de Lange, G., Wang, Z. H., Ristè, D., Dobrovitski, V. V., & Hanson, R. (**2010**). Universal dynamical decoupling of a single solid-state spin. Science, 330, 60–63. https://doi.org/10.1126/science.1192739.

[13] Neumann, P., Jakobi, I., Dolde, F., Burk, C., Reuter, R., Waldherr, G., Honert, J., Wolf, T., Brunner, A., Shim, J. H., Suter, D., Sumiya, H., Onoda, S., Isoya, J., & Wrachtrup, J. (**2013**). High-precision nanoscale temperature sensing using single defects in diamond. Nano Letters, 13, 2738–2742. https://doi.org/10.1021/nl401216y.

[14] Laraoui, A., & Meriles, C. A. (**2013**). Approach to dark spin cooling in a diamond nanocrystal. ACS Nano, 7, 3403–3410. https://doi.org/10.1021/nn400239n.

[15] Slichter, C. P. (**1990**). Principles of Magnetic Resonance, 3rd ed. Berlin, Germany: Springer.

[16] Abragam, A. (**1961**). The Principles of Nuclear Magnetism. Oxford, U.K.: Oxford University Press.

[17] Doherty, M. W., Manson, N. B., Delaney, P., Jelezko, F., Wrachtrup, J., & Hollenberg, L. C. L. (**2013**). The nitrogen-vacancy colour centre in diamond. Physics Reports, 528, 1–45. https://doi.org/10.1016/j.physrep.2013.02.001.

[18] Budker, D., & Jackson Kimball, D. F. (Eds.). (**2013**). Optical Magnetometry. Cambridge, U.K.: Cambridge University Press. https://doi.org/10.1017/CBO9780511846380.

[19] Degen, C. L. (**2008**). Scanning magnetic field microscope with a diamond single-spin sensor. Applied Physics Letters, 92, 243111. https://doi.org/10.1063/1.2943282.

[20] Datta, S., & Das, B. (**1990**). Electronic analog of the electro-optic modulator. Applied Physics Letters, 56, 665–667. https://doi.org/10.1063/1.102730.

[21] Žutić, I., Fabian, J., & Das Sarma, S. (**2004**). Spintronics: Fundamentals and applications. Reviews of Modern Physics, 76, 323–410. https://doi.org/10.1103/RevModPhys.76.323.

[22] Barry, J. F., Schloss, J. M., Bauch, E., Turner, M. J., Hart, C. A., Pham, L. M., & Walsworth, R. L. (**2020**). Sensitivity optimization for NV-diamond magnetometry. Reviews of Modern Physics, 92, 015004. https://doi.org/10.1103/RevModPhys.92.015004.

[23] Clarke, J., & Braginski, A. I. (Eds.). (**2004**). The SQUID Handbook: Fundamentals and Technology of SQUIDs and SQUID Systems. Weinheim, Germany: Wiley-VCH.

[24] Ripka, P. (**2000**). Magnetic Sensors and Magnetometers. Boston, MA, USA: Artech House.

 © Ariston Publications 2026. All rights reserved.